Electronic Supplementary Material (ESI) for Dalton Transactions.
This journal is © The Royal Society of Chemistry 2024

Electronic Supporting information

Factors Governing Protonation of Keggin-type Polyoxometalates: Influence of Core Structure in Clusters

Hiroshi Sampei[a], Hiromu Akiyama[a], Koki Saegusa[a], Masahiro Yamaguchi[a], Shuhei Ogo[b,c], Hiromi Nakai[d], Tadaharu Ueda[*b,c,e], and Yasushi Sekine[*a]

a. Department of Applied Chemistry, Waseda University, 3-4-1, Okubo, Shinjuku, Tokyo, 169-8555, Japan, E-mail ysekine@waseda.jp

b. Department of Marine Resource Science, Faculty of Agriculture and Marine Science, Kochi University, Nankoku783-8502, Japan

c. Marine Core Research Institute, Kochi University, Nankoku 783–8502, Japan

d. Department of Chemstry and Biochemistry, Waseda University, 3-4-1, Okubo, Shinjuku, Tokyo, 169-8555, Japan

e. MEDi center, Kochi University, Kochi 780-0842, Japan

This file includes:

Figs. S1 to S12

Tables S1 to S5

Other Supplementary Materials for this manuscript include the following:

.xyz and .chk files (ZIP)

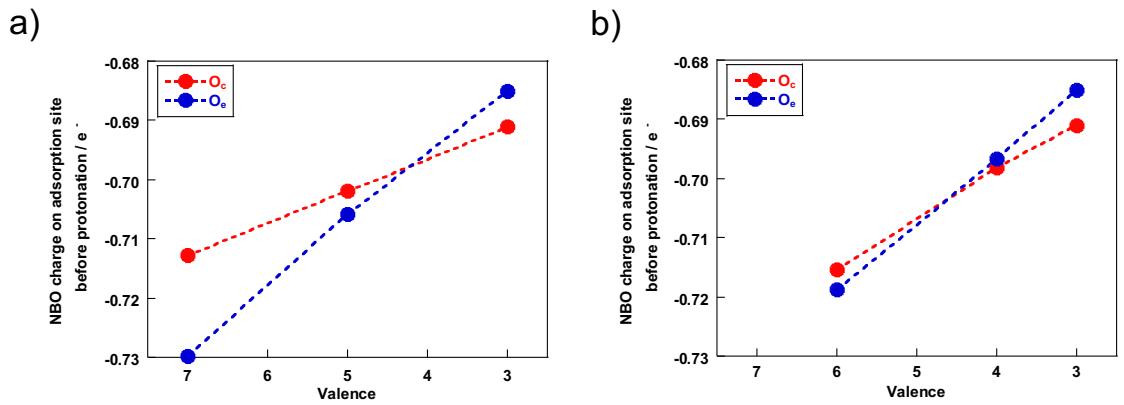

Figure S1. NBO charge on each adsorption site before protonation in α-PW12.

a) restricted DFT b) unrestricted DFT

The same trend of amount of charge change as Fig. 2 was observed in not only close shell systems but also open shell systems, indicates this trend of change of O_e and O_c occurs regardless of occupation.

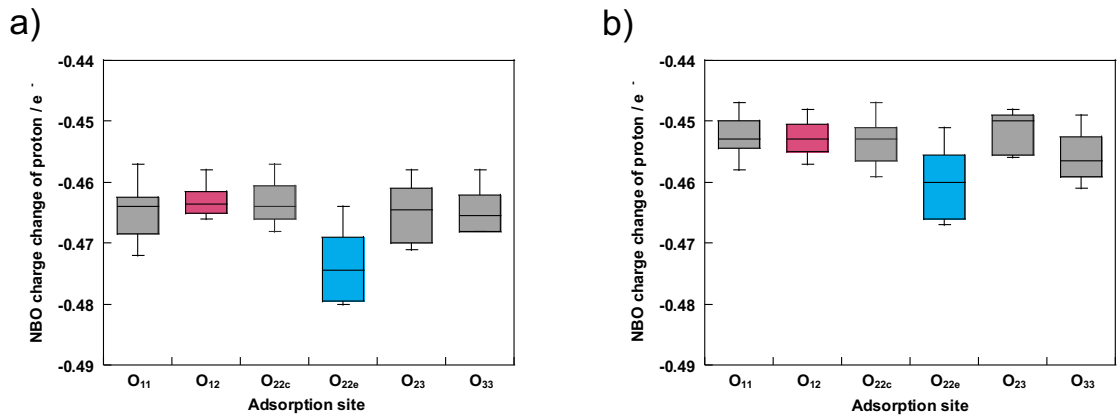

Figure S2 4 Box plot of NBO charge change of proton upon protonation in a) β-XMo12 and b) β-XW12. The upper and lower whiskers are set as the maximum and minimum values. The plots outside the whisker are outliers.

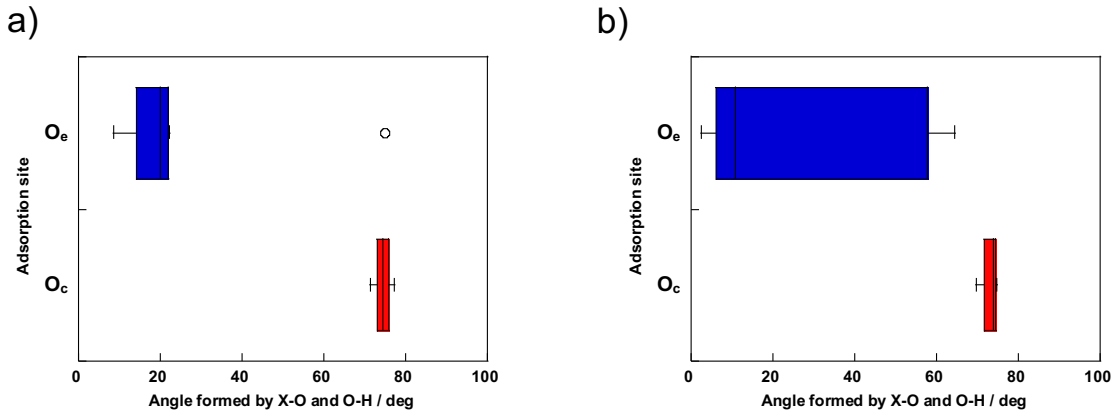

Figure S3 Box plot illustrating the relationship between adsorption site and protonation angles, angles between X-O and O-H, in a) α-XMo_{12} and b) α-XW_{12}. The upper and lower whiskers represent the maximum and minimum values. Outlying points outside the whisker are considered as outliers.

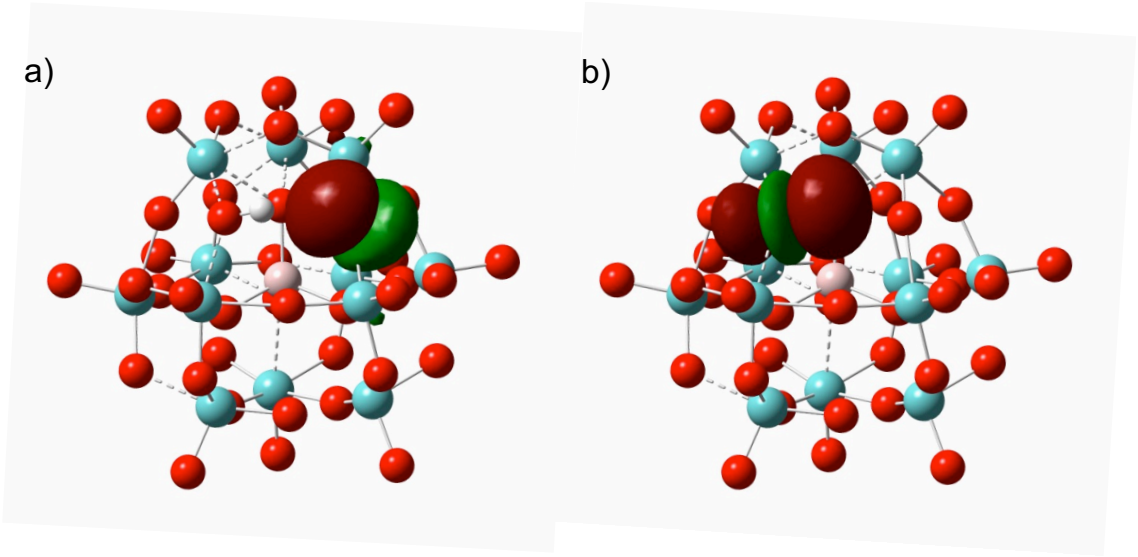

Figure S4 NBO orbitals of a) donor level and b) acceptor level for proton adsorption on O_{12} site in β-$AlMo_{12}$.

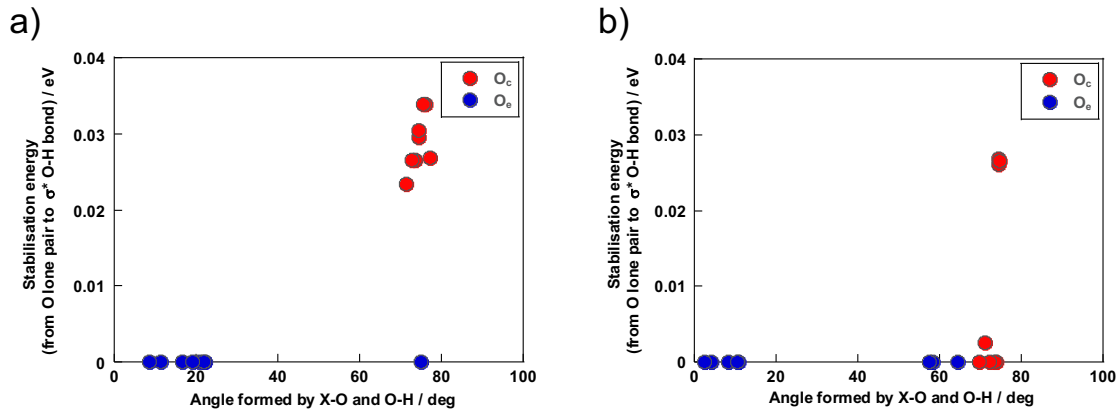

Figure S5 Relationship between stabilization energy and the protonation angles, angles between X-O and O-H, in a) α-XMo_{12} and b) α-XW_{12}.

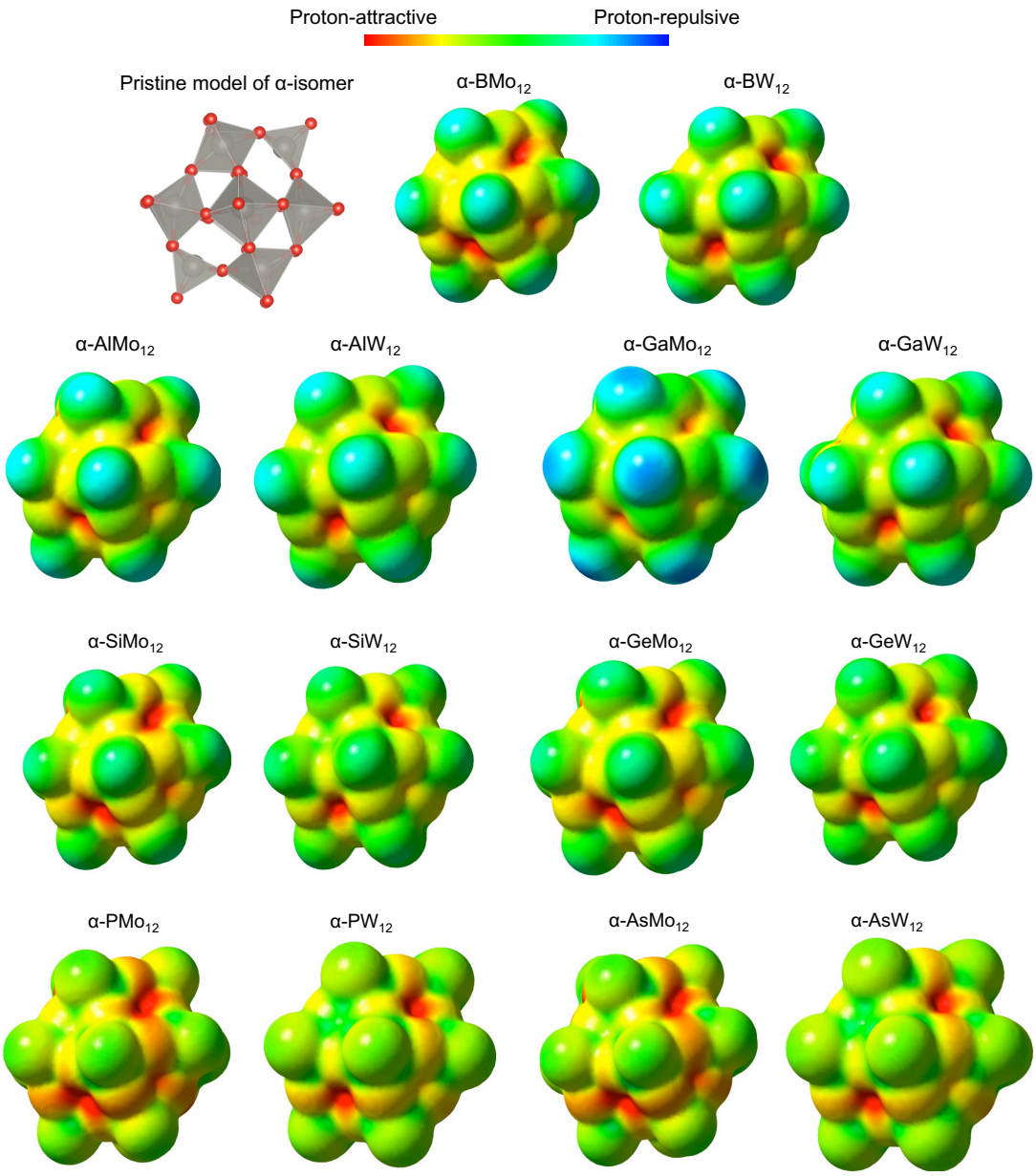
Proton-attractive
Proton-repulsive
Pristine model of α-isomer
α-BMo12
α-BW12
α-AlMo12
α-AlW12
α-GaMo12
α-GaW12
α-SiMo12
α-SiW12
α-GeMo12
α-GeW12
α-PMo12
α-PW12
α-AsMo12
α-AsW12

α-SMo_{12} α-SW_{12} Pristine model of β-isomer

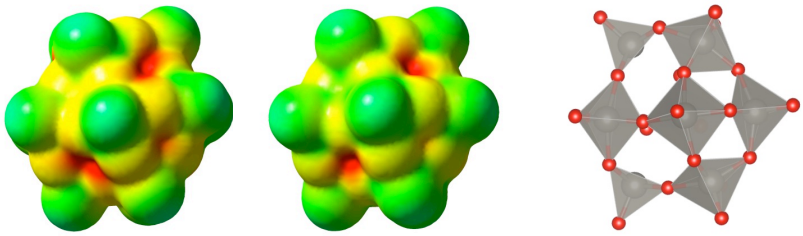

β-BMo_{12} β-BW_{12} β-$AlMo_{12}$ β-AlW_{12}

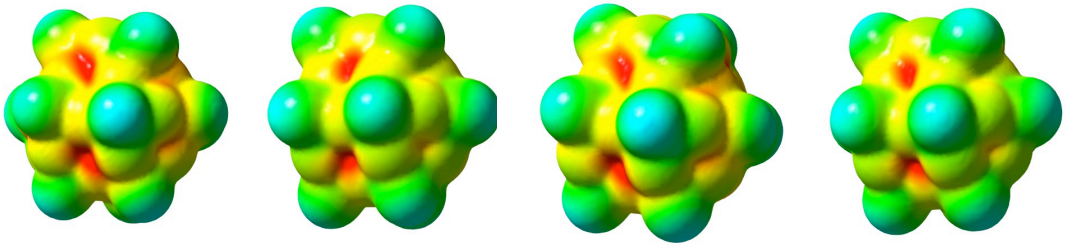

β-$GaMo_{12}$ β-GaW_{12}

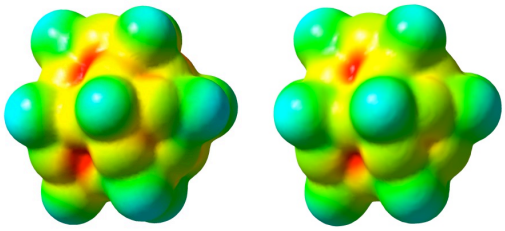

β-$SiMo_{12}$ β-SiW_{12} β-$GeMo_{12}$ β-GeW_{12}

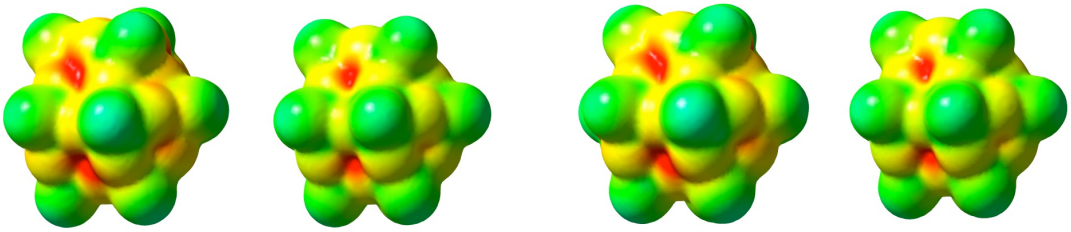

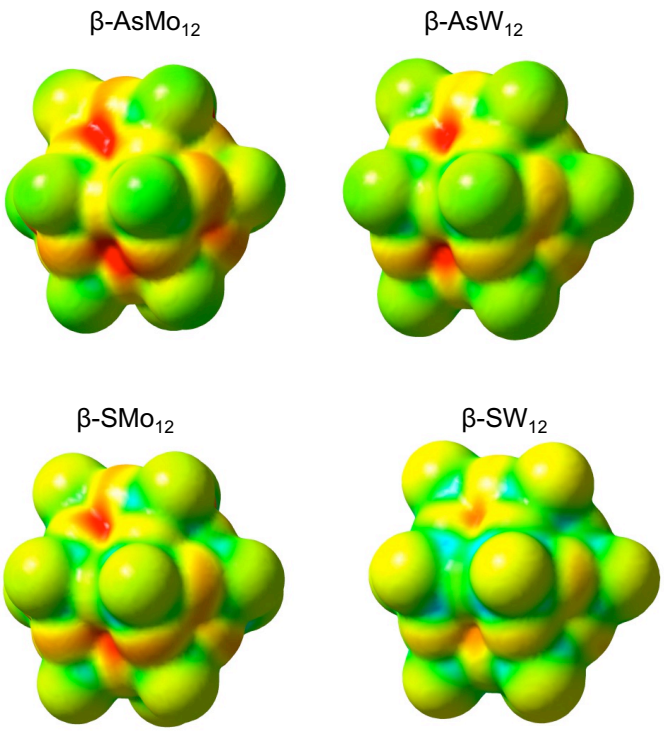

Figure S6 MEP mappings of α- and β- XM_{12} except for β-PM_{12}.

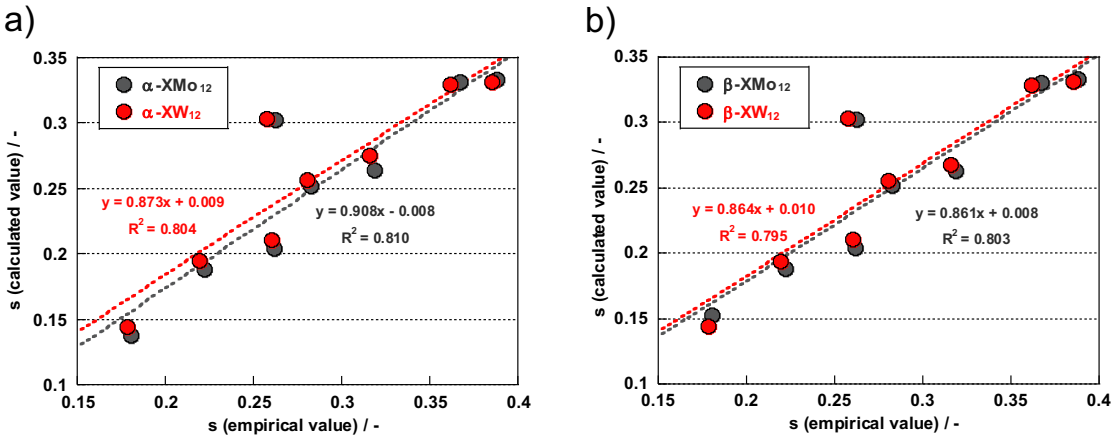

Figure S7 Correlation between empirical and calculated bond strength values on a) α-XM_{12} and b) β-XM_{12}.

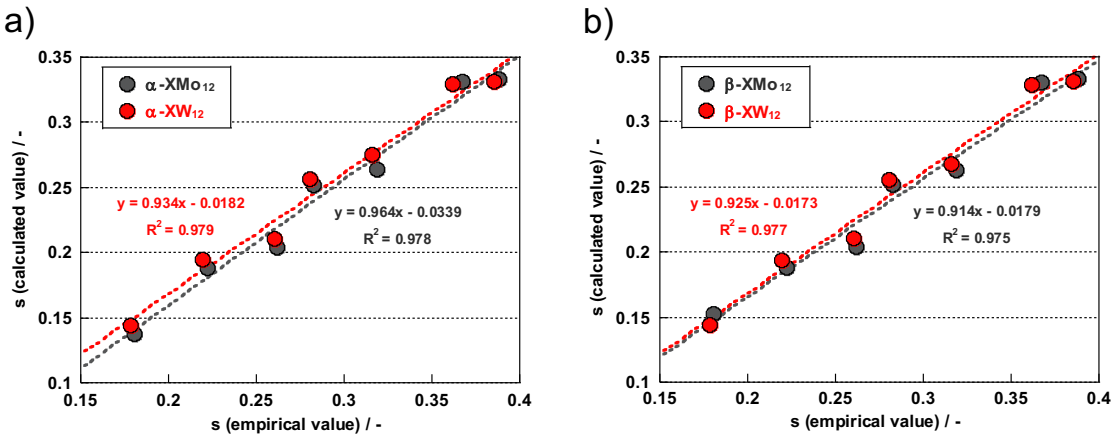

Figure S8 Correlation between empirical and calculated bond strength values except X=B a) on α-XM_{12} and b) on β-XM_{12}.

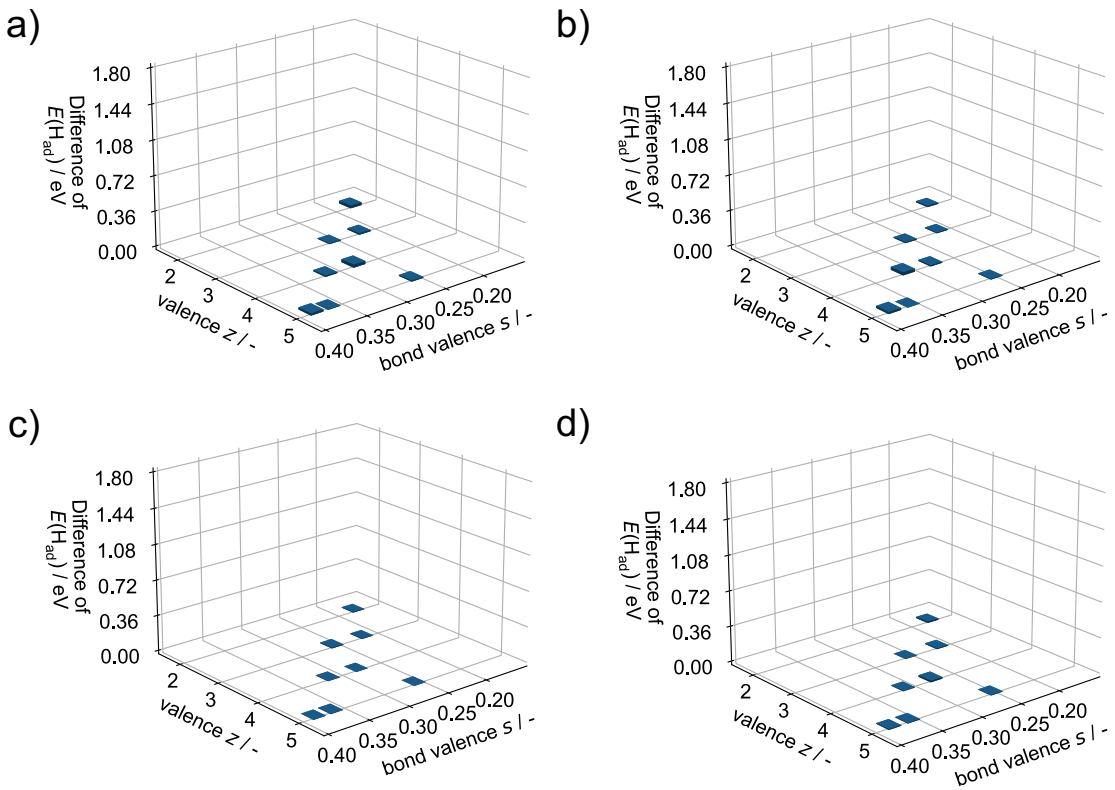

Figure S9 Absolute error of predicted protonation energy in a) α-XMo_{12}, b) α-XW_{12}, c) β-XMo_{12}, and d) β-XW_{12}. The width of axis corresponding to absolute error (from 0.0 to 1.8) is adjusted to the same as the drawn width of $E(H_{ad})$ in Fig. 8 (from -10.6 to -12.4).

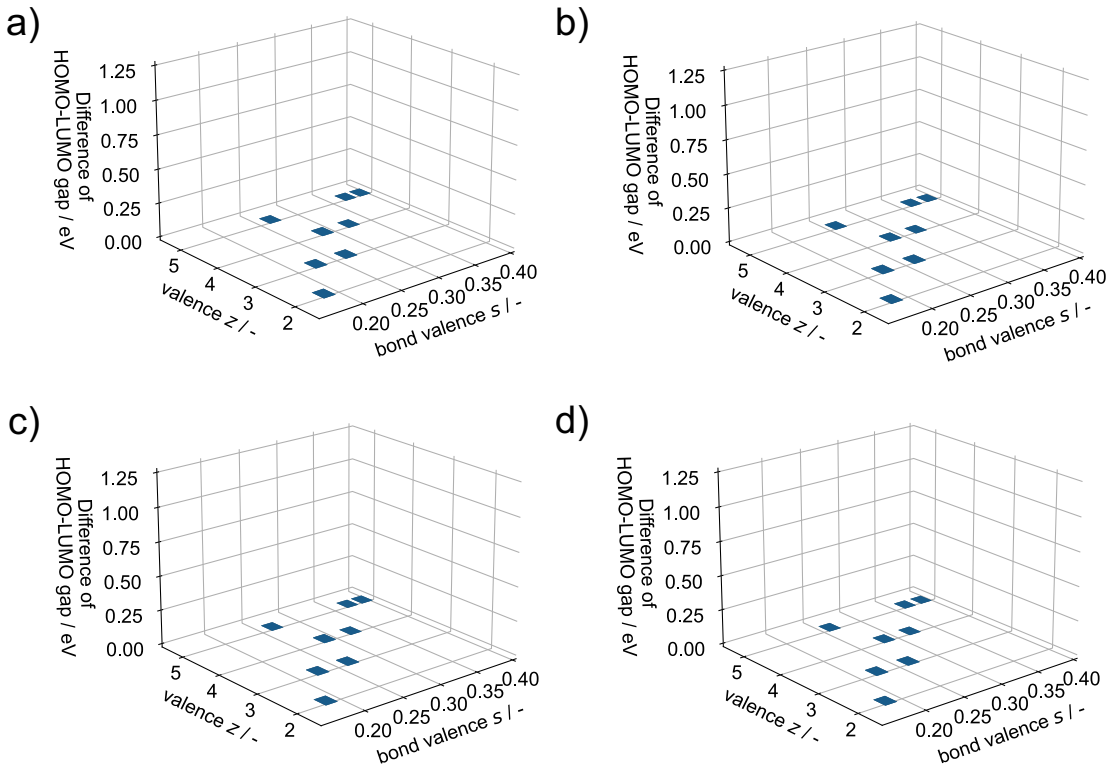

Figure S10 Absolute error of predicted HOMO-LUMO gap in a) α-XMo_{12}, b) α-XW_{12}, c) β-XMo_{12}, and d) β-XW_{12}. The width of axis corresponding to absolute error (from 0.0 to 1.25) is adjusted to the same as the drawn width of HOMO-LUMO gap in Fig. 9 (from 3.75 to 5.00).

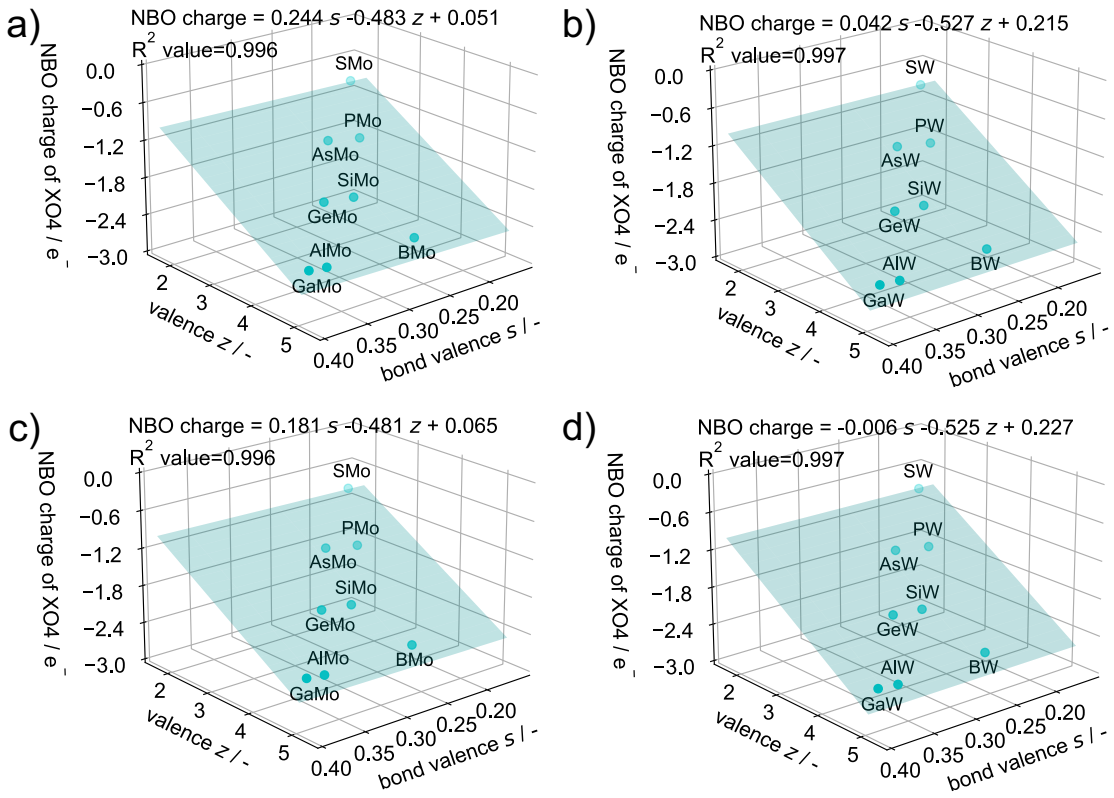

Figure S11 Regression of NBO charges of XO_4 core structure in a) α-XMo_{12}, b) α-XW_{12}, c) β-XMo_{12}, and d) β-XW_{12}.

We discuss that the valences of POM are derived from charges of XO_4 structure in main text. Moreover, we evaluate the NBO charges of XO_4 structures. The clear relationship between the NBO charges and governing factors for various responses suggests that the governing factors strongly involve degree of electron transfer from core structure to shell structure.

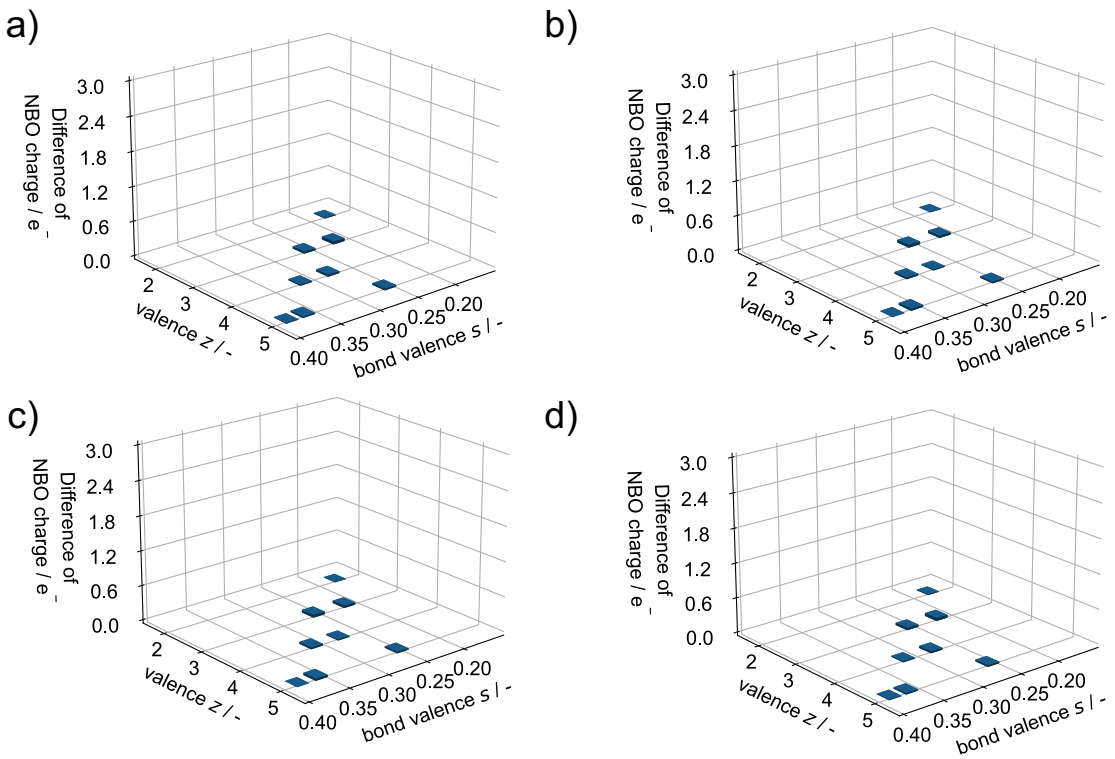

Figure S12 Absolute error of NBO charges of XO4 core structure in a) α-XMo_{12}, b) α-XW_{12}, c) β-XMo_{12}, and d) β-XW_{12}. The width of axis corresponding to absolute error (from 0.0 to 3.00) is adjusted to the same as the drawn width of NBO charge of XO_4 in Fig. S11 (from -3.00 to 0.00).

Table S1. Adsorption energies of each adsorption site A) M=Mo, B) M=W.

A)

X	z	α-isomer (eV)		β-isomer (eV)					
		H^+ on O_c	H^+ on O_e	H^+ on O_{11}	H^+ on O_{12}	H^+ on O_{22e}	H^+ on O_{22c}	H^+ on O_{23}	H^+ on O_{33}
B	5	-12.074	-12.134	-12.136	-12.213	-12.212	-11.978	-12.180	-12.144
Al	5	-12.151	-12.186	-12.192	-12.267	-12.219	-12.059	-12.232	-12.157
Ga	5	-12.178	-12.214	-12.217	-12.273	-12.226	-12.073	-12.254	-12.158
Si	4	-11.795	-11.796	-11.798	-11.927	-11.879	-11.679	-11.826	-11.847
Ge	4	-11.824	-11.834	-11.833	-11.947	-11.891	-11.708	-11.859	-11.857
P	3	-11.471	-11.423	-11.501	-11.598	-11.532	-11.340	-11.544	-11.545
As	3	-11.500	-11.465	-11.487	-11.615	-11.546	-11.370	-11.489	-11.556
S	2	-11.185	-11.128	-11.211	-11.293	-11.206	-11.034	-11.238	-11.256

B)

X	z	α-isomer (eV)		β-isomer (eV)					
		H^+ on O_c	H^+ on O_e	H^+ on O_{11}	H^+ on O_{12}	H^+ on O_{22e}	H^+ on O_{22c}	H^+ on O_{23}	H^+ on O_{33}
B	5	-11.961	-11.972	-11.958	-12.009	-12.039	-11.726	-11.955	-11.961
Al	5	-12.017	-12.056	-12.043	-12.088	-12.097	-11.832	-12.051	-12.026
Ga	5	-12.034	-12.095	-12.073	-12.102	-12.111	-11.852	-12.089	-12.037
Si	4	-11.650	-11.664	-11.649	-11.708	-11.680	-11.431	-11.635	-11.675
Ge	4	-11.671	-11.675	-11.679	-11.740	-11.726	-11.470	-11.685	-11.698
P	3	-11.303	-11.284	-11.302	-11.360	-11.320	-11.068	-11.288	-11.335
As	3	-11.357	-11.354	-11.317	-11.389	-11.349	-11.110	-11.324	-11.359
S	2	-10.979	-10.957	-10.969	-11.038	-10.991	-10.742	-10.987	-11.017

Table S2. Most favorable proton adsorption site using M06/Lanl2DZ level.

X	*z*	α-isomer		β-isomer	
		M=Mo	M=W	M=Mo	M=W
B	5	O_e	O_e	O_{22e}	O_{23}
Al	5	O_e	O_e	O_{22e}	O_{23}
Ga	5	O_e	O_e	O_{22e}	O_{23}
Si	4	O_e	O_e	O_{22e}	O_{22e}
Ge	4	O_e	O_e	O_{22e}	O_{22e}
P	3	O_e	O_e	O_{22e}	O_{12}
As	3	O_e	O_e	O_{22e}	O_{12}
S	2	O_e	O_e	O_{22e}	O_{12}

Table S3. HOMO-LUMO gap comparison of some Keggin POM.

Composition	Experimental value / eV	Calculated value / eV	Reported value / eV	reference
α-PW_{12}	3.5	4.7	2.7	[Gao 2015] [Hiskia 2001]
α-SiW_{12}	4.4	4.3	2.8	[Hiskia 2001]
α-PMo_{12}	3.9	4.8	-	[Hiskia 2001]

The reported values were referred to [López 2006].

Table S4. List of calculated HOMO-LUMO gaps

Composition	α-isomer / eV	β-isomer / eV
BMo_{12}	3.91	3.80
$AlMo_{12}$	4.59	4.51
$GaMo_{12}$	4.61	4.53
$SiMo_{12}$	4.40	4.32
$GeMo_{12}$	4.43	4.36
PMo_{12}	4.26	4.16
$AsMo_{12}$	4.28	4.20
SMo_{12}	4.15	4.02
BW_{12}	4.30	4.07
AlW_{12}	4.89	4.65
GaW_{12}	4.88	4.66
SiW_{12}	4.79	4.51
GeW_{12}	4.78	4.54
PW_{12}	4.70	4.45
AsW_{12}	4.68	4.44
SW_{12}	4.64	4.39

Table S5. Structural properties of α- and β-XM12 prior to proton adsorption

	α-isomer					β-isomer															
Model	d(X-O_A) (Å)	d(O_T-M) (Å)	d(M-O_A) (Å)	d(M-O_C) (Å)	d(M-O_T) (Å)	d(X-O_{Ad}) (Å)	d(O_{Td}-M) (Å)	d(X-O_{Ad}) (Å)	d(O_{Td}-M) (Å)	d(M-O_{11}) (Å)	d(M-O_{12}) (Å)	d(M-O_{12}) (Å)	d(M_t-O_{12}) (Å)	d(M_t-O_{23}) (Å)	d(M_d-O_{2a}) (Å)	d(M_d-O_{23}) (Å)	d(M_t-O_{23}) (Å)	d(M_t-O_{23}) (Å)	d(M_t-O_{3}) (Å)
BMo	1.532	2.402	1.945	1.927	1.710	1.539	2.396	1.535	2.401	1.950	1.710	1.934	1.932	1.917	1.959	1.711	1.943	1.948	1.925	1.709
AlMo	1.779	2.278	1.966	1.949	1.712	1.783	2.282	1.785	2.282	1.968	1.711	1.954	1.951	1.945	1.982	1.712	1.963	1.966	1.948	1.710
GaMo	1.834	2.257	1.972	1.953	1.712	1.837	2.261	1.839	2.263	1.975	1.711	1.957	1.954	1.951	1.992	1.713	1.968	1.971	1.951	1.711
SiMo	1.660	2.374	1.951	1.938	1.700	1.663	2.380	1.664	2.372	1.951	1.700	1.945	1.943	1.932	1.957	1.701	1.950	1.953	1.937	1.700
GeMo	1.750	2.330	1.959	1.946	1.701	1.753	2.337	1.754	2.331	1.959	1.701	1.951	1.950	1.940	1.966	1.702	1.957	1.960	1.944	1.700
PMo	1.568	2.464	1.943	1.934	1.690	1.568	2.472	1.571	2.458	1.943	1.690	1.941	1.940	1.926	1.943	1.690	1.944	1.945	1.933	1.690
AsMo	1.683	2.403	1.952	1.942	1.691	1.685	2.411	1.686	2.398	1.951	1.691	1.949	1.948	1.936	1.951	1.692	1.953	1.953	1.941	1.691
SMo	1.503	2.540	1.941	1.933	1.682	1.504	2.549	1.506	2.536	1.939	1.682	1.939	1.937	1.929	1.936	1.683	1.945	1.943	1.931	1.683
BW	1.528	2.419	1.934	1.918	1.727	1.534	2.414	1.534	2.413	1.934	1.727	1.925	1.921	1.910	1.936	1.728	1.935	1.937	1.917	1.727
AlW	1.767	2.293	1.952	1.937	1.729	1.770	2.296	1.772	2.291	1.947	1.728	1.938	1.935	1.929	1.948	1.729	1.948	1.952	1.931	1.728
GaW	1.821	2.270	1.957	1.942	1.729	1.822	2.275	1.825	2.269	1.951	1.729	1.940	1.938	1.933	1.952	1.729	1.952	1.956	1.934	1.728
SiW	1.656	2.387	1.941	1.929	1.718	1.657	2.393	1.660	2.383	1.939	1.718	1.935	1.932	1.924	1.940	1.719	1.942	1.943	1.928	1.718
GeW	1.742	2.343	1.946	1.934	1.719	1.744	2.350	1.747	2.340	1.945	1.719	1.939	1.937	1.931	1.944	1.720	1.947	1.949	1.932	1.719
PW	1.564	2.478	1.937	1.928	1.710	1.565	2.483	1.569	2.472	1.936	1.710	1.934	1.932	1.924	1.935	1.710	1.938	1.939	1.926	1.710
AsW	1.679	2.414	1.943	1.934	1.711	1.680	2.421	1.682	2.409	1.942	1.710	1.939	1.937	1.931	1.940	1.711	1.944	1.945	1.932	1.711
SW	1.502	2.554	1.936	1.929	1.704	1.501	2.560	1.504	2.548	1.934	1.703	1.935	1.934	1.927	1.932	1.704	1.938	1.938	1.927	1.704

	α-isomer					β-isomer															
Model	MO_tM (deg)	OMO_a (deg)	MO_aM (deg)	OMO_c (deg)	O_AXO_t (deg)	$O_{Ad}XO_{Td}$ (deg)	$O_{Td}XO_{Td}$ (deg)	$O_TM_tO_{11}$ (deg)	$O_TM_tO_{12}$ (deg)	$O_dM_tO_{12}$ (deg)	$O_dM_tO_{2a}$ (deg)	$O_dM_dO_{2a}$ (deg)	$O_dM_dO_{23}$ (deg)	$O_dM_tO_{23}$ (deg)	$O_dM_dO_{2a}$ (deg)	MO_1M_1 (deg)	$MO_{12}M_t$ (deg)	$M_tO_{23}M_d$ (deg)	$M_tO_{23}M_t$ (deg)	$M_tO_{3}M_t$ (deg)	$M_tO_{3}M_t$ (deg)
BMo	120.201	98.098	148.251	99.614	109.471	109.677	109.265	97.942	99.943	101.474	97.495	99.341	98.976	97.905	100.241	119.105	142.890	118.203	152.543	119.451	148.277
AlMo	117.039	98.047	151.854	100.519	109.471	109.463	109.480	97.778	100.545	101.796	97.483	99.740	98.814	97.911	100.784	117.125	145.695	115.143	156.381	116.739	151.940
GaMo	116.794	98.076	152.374	100.664	109.471	109.393	109.549	97.646	100.779	102.002	97.351	99.785	98.822	97.939	100.465	116.917	146.173	114.604	156.639	116.614	152.584
SiMo	122.278	99.744	151.632	101.486	109.471	109.608	109.335	99.638	101.567	101.567	99.478	100.975	100.610	99.614	101.733	121.969	146.025	119.891	157.909	121.405	151.727
GeMo	121.138	99.753	152.786	101.770	109.471	109.591	109.321	99.581	101.778	102.883	99.358	101.189	100.634	99.624	101.930	147.102	146.569	116.983	158.831	120.609	152.812
PMo	127.146	101.505	152.083	102.702	109.471	109.700	109.242	101.399	102.827	103.649	101.159	102.449	102.321	101.431	102.868	126.912	146.911	124.026	160.074	126.093	152.134
AsMo	125.685	101.448	153.399	102.908	109.471	109.673	109.269	101.337	102.940	103.867	101.195	102.644	102.164	101.363	103.072	125.654	147.801	122.936	161.198	124.723	153.471
SMo	131.584	103.423	153.266	104.173	109.471	109.793	109.148	103.045	104.296	104.864	102.651	104.145	104.195	103.379	104.107	131.441	147.663	127.524	162.935	131.473	152.868
BW	122.160	99.216	148.513	100.612	109.471	109.754	109.187	99.353	100.683	101.645	99.256	99.988	100.434	99.083	100.818	121.312	143.453	119.770	154.948	121.892	148.502
AlW	119.107	99.137	151.991	101.428	109.471	109.801	109.140	99.195	101.624	102.335	99.212	101.019	100.316	99.005	101.631	119.394	146.123	117.663	158.759	119.400	151.877
GaW	118.825	99.127	152.578	101.685	109.471	109.831	109.109	99.132	101.925	102.556	99.216	101.383	100.262	99.000	101.878	119.299	146.649	117.448	159.559	119.145	152.429
SiW	123.923	100.863	151.962	102.204	109.471	109.665	109.276	100.799	102.242	103.042	100.585	101.973	101.743	100.728	102.319	123.886	146.475	121.401	159.781	123.771	151.928
GeW	123.060	100.901	152.985	102.500	109.471	109.745	109.196	100.784	102.575	103.289	100.608	102.185	101.728	100.715	102.582	123.244	147.315	120.756	160.842	123.000	152.961
PW	128.698	102.414	152.397	103.217	109.471	109.708	109.234	102.287	103.355	104.095	101.806	103.215	103.289	102.355	103.340	128.447	147.388	125.100	161.518	128.298	152.308
AsW	127.265	102.413	153.647	103.496	109.471	109.760	109.181	102.274	103.586	104.299	101.787	103.568	103.190	102.326	103.563	127.226	148.280	124.141	162.544	126.949	154.567
SW	133.002	104.002	153.556	104.636	109.471	109.808	109.132	103.836	104.714	105.629	102.802	104.937	104.740	103.989	104.580	132.772	148.714	128.573	163.997	132.800	153.077

Table S6. Comparison of differential energies of protonation between experimental and calculated values.

Composition	$\log(\frac{[HXM_{12}]}{[XM_{12}][H^+]})$	$\log(\frac{[\alpha\text{–}HXM_{12}]}{[\alpha\text{–}XM_{12}][H^+]})$	ΔG from α-PM_{12} (experimental) / eV	ΔG from α-PM_{12} (calculated) / eV	reference
β-PW_{12}	1.176	1.398	0.013	-0.057	[Ueda 2017]
SMo_{12}	5.6	12.7	0.420	0.286	[Himeno 2005]
$GeMo_{12}$	21.1	12.7	-0.497	-0.363	[Himeno 2005]
GeW_{12}	14.2	5.6	-0.509	-0.372	[Himeno 2005]
BW_{12}	22.3	5.6	-0.988	-0.669	[Himeno 2005]

The protonation energies were compared by differences from that of α-PM_{12} since equation (1) does not include the interaction between a proton and the solvent, acetonitrile, and does not calculate correct absolute protonation energies. Considering stability and abundance of each isomer, Gibbs energies of α-isomers were used in the cases of no mention of isomer in a reference. These comparisons showed that the Gibbs energies of experiment and calculation are almost confident.

References in this SI

[Gao 2015] L.-H. Gao, J.-F. Zhang, H.-L. Wang, X.-Y. Lin, J.-M. Qi, K.-Z. Wang, *Electrochim. Acta* 2015, **166**, 215–222.

[Hiskia 2001] A. Hiskia, A. Mylonas and E. Papaconstantinou, *Chem. Soc. Rev.* 2001, **30**, 62–69.

[López 2006] X. López, J. A. Fernández and J. M. Poblet, *Dalton Trans.* 2006, 1162–1167.

[Shahrnoy 2018] A. A. Shahrnoy, A. R. Mahjoub, A. Morsali, M. Dusek and V. Eigner, *Ultrasonics Sonochemistry* 2018, **40**, 174–183.

[Ueda 2017] T. Ueda, K. Kodani, H. Ota, M. Shiro, S.-X. Guo, J. F. Boas, A. M. Bond, *Inorg. Chem.* 2017, **56**, 7, 3990–4001.

[Himeno 2005] S. Himeno, M. Takamoto, R. Santo, A. Ichimura, *Bull. Chem. Soc. Jpn.* 2005, **78**, 95–100.